Towards Image-Dependent Safety Hulls for Fiber Tracking

S. Barbieri[1], J. Klein[1], C. Nimsky[2], and H. K. Hahn[1]
[1]Fraunhofer MEVIS - Institute for Medical Image Computing, Bremen, Germany, [2]Department of Neurosurgery, University Marburg, Marburg, Germany

Introduction: The evaluation of fiber tracking algorithms is a challenging problem, given that software or hardware models are needed in order to have a ground truth to compare against (see for example [1-3]). In this work we introduce a novel global precision measure for tracked fibers, the "safety radius". We make use of a software model in order to systematically analyze the influence of image noise, fiber bundle diameter, number of seed points and tensor anisotropy on the safety radius. The latter is used to construct safety hulls, i.e. tubes that surround the tracked fibers and indicate their margin of error. Finally, we analyze the spatial distribution of tracked fibers.

Methods: Our software model is given by a portion of a torus generated using a solid kernel as described in [4], which is used to compute a set of synthetic diffusion weighted images (DWI), see an example image shown in Fig. 1(a). The DW signal is computed according to the CHARMED model proposed in [5,6], where we restrict ourselves to the hindered model. We assume cylindrically symmetric tensors and for the fiber bundle we set the eigenvalues of the diffusion tensors parallel and perpendicular to the axonal fibers (denoted by $\lambda_{\parallel}$ and $\lambda_{\perp}$ respectively) to values that are compatible with eigenvalues of tensors encountered in white matter, based on reports from [7,8]. For the background we use isotropic tensors. Partial volume effects are modeled by sampling the image at $(0.1\text{mm})^3$ and then linearly resampling it at $(1\text{mm})^3$. Image noise is simulated by adding Rice distributed noise to the DW images as in [9]. The DW images are used to compute the tensor valued images. The seed ROI used for fiber tracking is set as a circle located on a plane perpendicular to the fiber bundle, with the same diameter as the cross section of the fiber bundle (see Fig. 1(a)). For fiber tracking, we use the advection-diffusion based algorithm presented in [10].

To evaluate our fiber tracking results, we determine a so called safety radius r_s. Given a cross section of the tracked fiber bundle, the safety radius is defined as the minimal radius that is needed so that if a circle with radius r_s were placed around each fiber tracked inside the bundle, the aggregate of these circles would form a topological cover of the cross section of the modeled fiber bundle. In order to find r_s, we first compute the Voronoi Diagram of the points inside the cross section of the fiber bundle; r_s is then given by the maximal distance between one such point and the borders of the corresponding cell (see Fig. 1(b)). Finally, we are interested in the spatial distribution of the tracked fibers, which we analyze by looking at cross sections of the fiber bundle. We partition the cross section into six semi-annuli of equal area as shown in Fig. 1(c). At each cross section, we count how many fibers lie in each part.

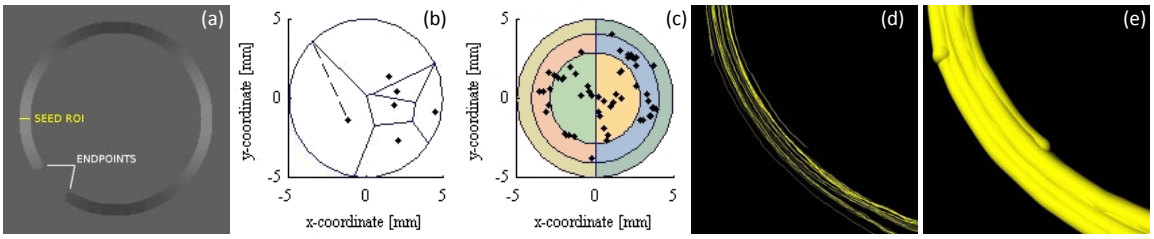

Figure 1: (a): DW image of a synthetic fiber bundle, gradient in x direction, with overlayed seed ROI shown in yellow. (b): Cross section of the tracked fiber bundle (location of fibers shown as dots) and the corresponding Voronoi Diagram. The length of the dashed black line segment corresponds to the safety radius. (c): Partitioned cross section of the tracked fiber bundle. Fibers with positive x-coordinate are on the interior of the circular fiber path. (d): A portion of a tracked fiber bundle. (e): Same portion of a tracked fiber bundle as in (d) but with a 3mm safety hull around each fiber.

Results: In order to generate the software model and to determine the DW images we use the following values as default parameters. Gradient strength: 20T/m, pulse width: 35msec, diffusion time: 40msec, radius of fiber bundle path: 80mm, diameter of bundle cross section: 10mm, $\lambda_{\parallel}$ for the bundle: $11.3 \cdot 10^{-4}$ mm²/s, $\lambda_{\perp}$ for the bundle: $5.15 \cdot 10^{-4}$ mm²/s, $\lambda_{\parallel} = \lambda_{\perp}$ for the background: $9.9 \cdot 10^{-4}$ mm²/s, thermal noise variance: 1.5. Voxel size is $(1\text{mm})^3$, the distance between seed points 1mm and we use 6 different gradient directions. Statistical computations are performed every 10mm of arc length, going counterclockwise from $180°$. We perform four separate experiments in which we vary one of the following parameters: the thermal noise variance between 0 and 6, by a step of 0.2, the diameter of the bundle cross section from 5 to 15mm, by a step of 1mm, the distance between seed points between 0.4 and 3mm, by a step of 0.2mm, $\lambda_{\perp}$ of the fiber bundle from 5.15 to $11.35 \cdot 10^{-4}$ mm²/s, by a step of $0.2 \cdot 10^{-4}$ mm²/s. For each set of parameters we repeat the addition of noise, followed by tracking and statistical computations, 100 times. Fig.2 shows the maximal safety radius plots after tracking 20cm for the different experiments.

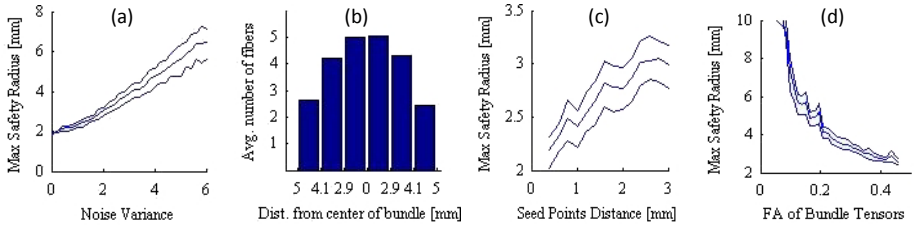

Figure 2: (a): Dependence of the maximal safety radius on noise variance. Lines correspond to median, upper and lower quartile. (b): Overall averaged number of fibers in the different plane parts. Bars on the left correspond to fibers on the exterior of the circular fiber path, bars on the right correspond to fibers on the interior. (c): Safety radius vs. distance between seed points. (d): Safety radius vs. fractional anisotropy.

Conclusions: The plot of noise variance vs. safety radius (Fig.2(a)) suggests that for the analyzed images in which the noise variance is below 2 using a safety hull with 3mm radius is appropriate (for bundles of up to 20cm length). Fig.2(b) shows that on average, there are approximately half as many fibers located on the outer third of the bundle's cross section than on the inner third, given that they are the first to leave the bundle. There isn't a significant difference between the number of fibers on the interior portion of the fiber bundle path and on its exterior. The diameter of the fiber bundle does not seem to overly impact fiber tracking results. As expected, a larger number of seed points corresponds to a smaller safety radius. The oscillations in the plot of Fig.2(c) are likely due to having seed points closer or further away from the border of the bundle. Fig.2(d) indicates that the deflection based algorithm works well if the fractional anisotropy of the "white matter" tensors is above 0.25, which should be the case for fiber bundles that do not cross. With this paper, we have gained some insight on the relationship between noise, fiber bundle diameter, number of seed points, tissue anisotropy, and the margin of error of fiber tracking. Further tests are necessary, for example using probabilistic fiber tracking approaches, to get a more complete picture. Moreover, we could apply the gained knowledge about the magnitude of fiber tracking errors to improve existing fiber tracking algorithms.

References: [1] N.F.Lori et al., *NMR in Biomedicine*, Vol. 15, pp.493-515, 2002 [2] C.Goessel et al., *NeuroImage*, Vol. 16, pp.378-388, 2001 [3] E.Fieremans et al., *Journal of Magnetic Resonance*, Vol. 190(1), pp.189-199, 2008 [4] A.Leemans et al., *Magnetic Resonance in Medicine*, Vol. 53, pp. 944-953, 2005 [5] Y.Assaf et al., *Magnetic Resonance in Medicine*, Vol. 52, pp. 965-978, 2004 [6] Y.Assaf et al., *NeuroImage*, Vol. 27, pp. 48-58, 2005 [7] C.Pierpaoli et al., *Radiology*, Vol. 201, pp. 637-648, 1996 [8] Y.A.Bhagat et al., *Magnetic Resonance Imaging*, Vol. 20, pp. 216-227, 2004 [9] H.K.Hahn et al., *Acta Neurochirurgica*, Suppl. 98, pp. 33-41, 2006 [10] M.Schlüter et al., *SPIE Medical Imaging*, Vol. 5746, pp. 836-844, 2005